Electronic Supplementary Material (ESI) for Nanoscale.

Nanoscale RSCPublishing

PAPER

Supporting Information

Enhanced Second Harmonic Generation of MoS_2 Layers on a Thin Gold Film

Jianhua Zeng,[a] Maohui Yuan,[a] Weiguang Yuan,[a] Qiaofeng Dai,[a] Haihua Fan,[a] Sheng Lan*[a] and Shaolong Tie*[b]

SI-1. Experimental setup

The experimental setup used to characterize the nonlinear optical responses of MoS_2 layers is schematically shown in Fig. S1. The femtosecond (fs) laser light with a duration of 130 fs and a repetition rate of 76 MHz delivered by a fs oscillator (Mira900S, Coherent) was introduced into an inverted microscope (Axio Observer A1, Zeiss). It was reflected by using a dichroic mirror and focused by using the 60× objective on the MoS_2 layers. A combination of a half-wavelength plate and a quarter-wavelength plate was employed to adjust the polarization of the fs laser light on the excitation plane. The nonlinear optical signals were collected by using the same objective and directed to a spectrometer (SR-500i-B1, Andor) equipped with a charge coupled device (DU970N, Andor) for analysis.

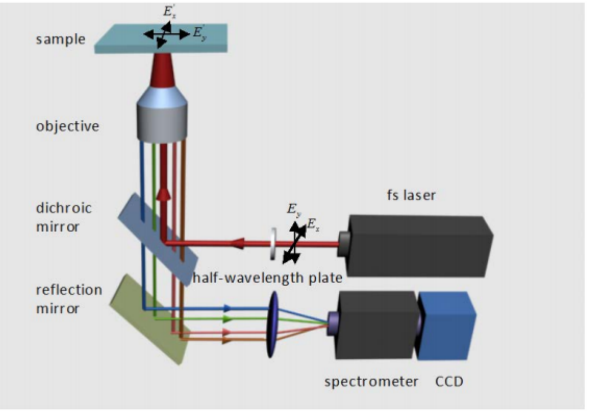

Fig. S1 Experimental setup used to characterize the nonlinear optical responses of the MoS_2 layers on the SiO_2/Si and Au/SiO_2 substrates.

SI-2. Complex refractive indexes of single-layer (1L) and bulk MoS_2 used in the calculation

In our case, the complex refractive index of bulk MoS_2 used in the FDTD simulation was derived from the complex dielectric constants reported previously by using the following relationship:[S1]

$$\begin{cases} \varepsilon_1 = n^2 - k^2 \\ \varepsilon_2 = 2nk \end{cases} \tag{S1}$$

Based on Eqn S1, one can easily obtain

$$\begin{cases} n = \sqrt{\dfrac{\varepsilon_1 + \sqrt{\varepsilon_1^2 + \varepsilon_2^2}}{2}} \\ k = \dfrac{\varepsilon_2}{\sqrt{2\varepsilon_1 + 2\sqrt{\varepsilon_1^2 + \varepsilon_2^2}}} \end{cases} \tag{S2}$$

where ε_1 and ε_2 are the real and imaginary parts of the complex dielectric constant and n and k are the real and imaginary parts of the complex refractive index. The photon energy is converted to photon wavelength according to the following relationship:

$$\lambda = \frac{1240}{E} \tag{S3}$$

Here, the unit for energy is eV while that for wavelength is nm. The complex refractive indexes for single-layer and bulk MoS_2 in the wavelength region of 380-730 nm are presented in Fig. S2.[S2]

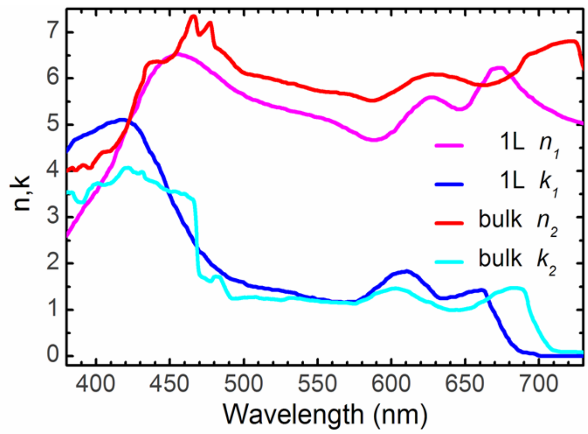

Fig. S2 Real and imaginary parts of the complex refractive indexes of single-layer and bulk MoS_2 used in the FDTD simulation.

SI-3. Comparison of the reflection spectra calculated by using the complex refractive indexes of single-layer and bulk MoS_2

In order to find the influence of the complex refractive index on the calculated reflection spectra, we have calculated the reflectance spectrum of single-layer MoS_2 on the Au/SiO_2 substrate by using the complex refractive indexes of single-layer and bulk MoS_2. A comparison of the two reflection spectra is presented in Fig. S3. It can be seen that the difference between the two reflection spectra is too small to induce any difference in the chromaticity coordinate. For this reason, we simply adopted the complex refractive index of bulk MoS_2 in all the reflection spectra calculations described in this work.

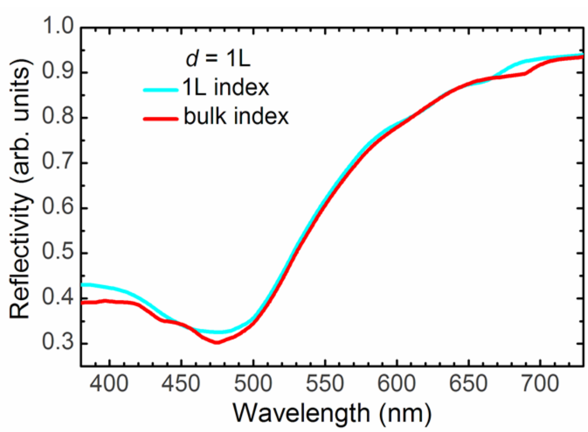

Fig. S3 Comparison of the reflection spectra calculated for single-layer MoS_2 on the Au/SiO_2 substrate by using the complex refractive indexes of single-layer and bulk MoS_2.

SI-4. Calculation of chromaticity coordinates

Based on the theory of colorimetry, the color of an object can be described by its tristimulus values (X, Y, and Z) which are related with the chromaticity coordinates (x, y, and z) by the following Eqn:[S3]

$$\begin{cases} X = k\int_{\lambda} S(\lambda)\bar{x}(\lambda)\beta(\lambda)\,\mathrm{d}\lambda \\ Y = k\int_{\lambda} S(\lambda)\bar{y}(\lambda)\beta(\lambda)\,\mathrm{d}\lambda \\ Z = k\int_{\lambda} S(\lambda)\bar{z}(\lambda)\beta(\lambda)\,\mathrm{d}\lambda \\ x = X / X+Y+Z \\ y = Y / X+Y+Z \\ z = Z / X+Y+Z \end{cases} \quad . \tag{S4}$$

Here, $S(\lambda)$ is the relative power of the illumination at wavelength λ, $\bar{x}(\lambda)$, $\bar{y}(\lambda)$, $\bar{z}(\lambda)$ are the color matching functions for the CIE 1931 2° Standard Observer, $\beta(\lambda)$ is the spectral reflectivity of the sample at wavelength λ.

The photos of the MoS_2 sheets on the Au/SiO_2 substrate were taken through the eyepieces of a microscope. A blue filter was used and the spectrum of the illumination light in the wavelength region of 380-730 nm is shown in Fig. S4. It was used as the spectrum of the light source in the calculation of chromaticity coordinates.

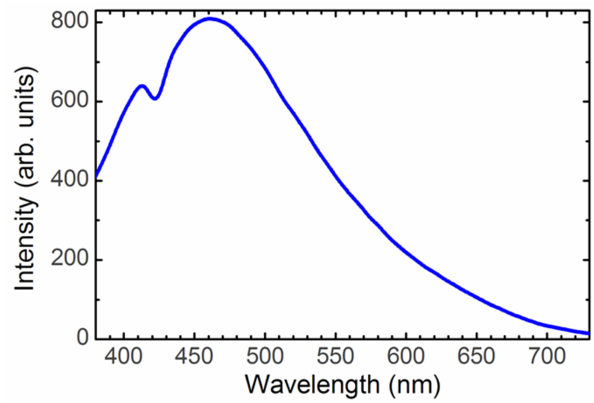

Fig. S4 Spectrum of the illumination light used in the microscope and also in the calculation of the chromaticity coordinates of the MoS_2 layers on the Au/SiO_2 substrate.

Based on the reflection spectra calculated by using the FDTD simulation, we can easily derive the corresponding chromaticity coordinates for the MoS_2 layers with different thicknesses on the Au/SiO_2 substrate, as shown in Table S1.

Table S1 Chromaticity coordinates derived for the MoS_2 layers with different thicknesses on the Au/SiO_2 substrate based on their calculated reflection spectra.d is thicknesses of the MoS_2 layer.

d (nm)	x	y	d (nm)	x	y
0.65 (1L)	0.288	0.329	8	0.152	0.131
1.30 (2L)	0.297	0.323	9	0.155	0.153
1.95 (3L)	0.300	0.302	10	0.162	0.174
2.60 (4L)	0.295	0.266	15	0.196	0.234
3.25 (5L)	0.279	0.223	17	0.204	0.246
3.50	0.271	0.205	18	0.208	0.251
3.90 (6L)	0.256	0.179	20	0.213	0.259
4	0.253	0.173	25	0.223	0.274
4.55 (7L)	0.230	0.143	30	0.232	0.282
5	0.211	0.124	35	0.238	0.278
6	0.177	0.106	40	0.239	0.261
7	0.157	0.112	50	0.219	0.221

SI-5. Measurements of Raman scattering spectra

We measured the Raman scattering spectra for the MoS_2 layers with different thicknesses on the Au/SiO_2 substrate and they are presented in Fig. S5.

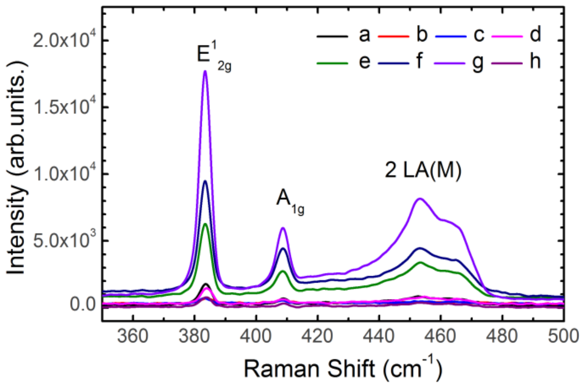

Fig. S5. Raman scattering spectra measured for the MoS_2 layers with different thicknesses on the Au/SiO_2 substrate.

SI-6. Calculation of the enhancement factors for electric field intensity and SHG in the MoS_2 layers

We have employed the FDTD simulation to calculate the electric field intensity distributions in the MoS_2 layer with different thicknesses on both the SiO_2/Si and Au/SiO_2 substrates and obtained the enhancement factors of the electric field intensity at both the fundamental light and the second harmonic, as shown in Table S3 and S4. The complex refractive indexes of MoS_2,[S1,S2] Au,[S4] SiO_2, and Si used in the FDTD simulation are summarized in Table S2.[S5] The enhancement factors for SHG can be derived by using Eqn (1) in the text and also presented in Tables S3 and S4. For both the SiO_2/Si and Au/SiO_2 substrates, the enhancement factors for SHG are normalized by using the enhancement factor of single-layer MoS_2 as reference.

Table S2 Complex refractive indexes of MoS_2 (including single-layer and bulk MoS_2), Au, SiO_2 and Si used in the calculation of the electric field intensity distributions in the MoS_2 layers with different thicknesses on the SiO_2/Si and Au/SiO_2 substrates.

	λ	indexes			λ	indexes	
	(nm)	n	k		(nm)	n	k
1L MoS_2	800	4.626	0	SiO_2	800	1.450	0
	400	3.544	4.890		400	1.470	0
bulk MoS_2	800	5.392	0.058	Si	800	3.681	0.005
	400	4.252	3.725		400	5.587	0.303
Au	800	0.154	4.895				
	400	1.469	1.953				

Table S3 Enhancement factors in electric field intensity ($|E|^2$) at the fundamental light (800 nm) and the second harmonic (400 nm) and the enhancement factors (EF) in SHG calculated for MoS_2 layers with different thicknesses on the Au/SiO_2 substrate. d is thicknesses of the MoS_2 layer.

d (nm)	E^2_{max} at λ_{ex}		EF_{abs}	EF_{nor}	d (nm)	E^2_{max} at λ_{ex}		EF_{abs}	EF_{nor}
	800 nm	400 nm				800 nm	400 nm		
0.65 (1L)	2.226	1.760	8.721	1	15	31.365	0.162	159.370	18.274
1.95 (3L)	2.830	0.559	4.477	0.513	16	36.545	0.151	201.666	23.124
3.25 (5L)	3.425	0.465	5.455	0.626	17	37.688	0.147	208.797	23.942
3.50	3.564	0.451	5.729	0.657	18	36.206	0.143	187.455	21.495
4	3.859	0.424	6.314	0.724	19	32.543	0.140	148.267	17.001
4.55 (7L)	4.194	0.394	6.930	0.795	20	27.719	0.138	106.031	12.158
5	4.733	0.365	8.176	0.938	21	22.768	0.137	71.018	8.143
6	5.581	0.325	10.123	1.161	22	18.465	0.137	46.711	5.356
7	6.615	0.292	12.777	1.465	23	15.118	0.137	31.312	3.590
8	7.886	0.264	16.418	1.883	24	12.532	0.138	21.673	2.485
9	9.459	0.241	21.563	2.473	25	10.599	0.139	15.615	1.791
10	12.280	0.216	32.572	3.735	30	5.344	0.145	4.141	0.475
11	14.959	0.201	44.978	5.157	35	3.258	0.150	1.592	0.183
12	18.261	0.188	62.691	7.189	40	2.337	0.153	0.836	0.096
13	22.218	0.178	87.868	10.075	50	1.688	0.154	0.439	0.050
14	26.709	0.169	120.560	13.824					

Table S4 Enhancement factors in electric field intensity at the fundamental light (800 nm) and the second harmonic (400 nm) and the enhancement factors in SHG calculated for MoS_2 layers with different thicknesses on the SiO_2/Si substrate.*d* is thicknesses of the MoS_2 layer.

d (nm)	E^2_{max} at λ_{ex}		EF_{abs}	EF_{nor}	*d* (nm)	E^2_{max} at λ_{ex}		EF_{abs}	EF_{nor}
	800nm	400nm				800nm	400nm		
0.65 (1L)	2.308	2.483	13.223	1	20	2.506	0.129	0.81	0.061
1.95 (3L)	3.141	0.666	6.571	0.497	25	2.052	0.133	0.56	0.042
3.25 (5L)	3.358	0.566	6.382	0.483	30	1.738	0.14	0.423	0.032
4.55 (7L)	3.437	0.456	5.387	0.407	35	1.543	0.146	0.348	0.026
5	3.456	0.401	4.79	0.362	40	1.445	0.148	0.309	0.023
10	3.436	0.210	2.479	0.187	50	1.491	0.148	0.329	0.025
15	3.073	0.152	1.435	0.109					

SI-7. Evolution of SHG intensity with increasing ablation time

As mentioned in the manuscript, we can use fs laser light with sufficiently large excitation intensity to ablate the MoS_2 layers. With decreasing thickness, the SHG intensity is also changed with ablation time. In experiments, we recorded the nonlinear response spectrum of a MoS_2 layer after every 30 s and the evolution of the nonlinear response spectrum with increasing ablation time is shown in Fig. S6(A). In Fig. S6(B), we plot the dependence of the SHG intensity on the ablation time. In this case, a monotonic reduction in the SHG intensity is observed, implying that the initial thickness of the MoS_2 layer is close to 17 nm.

In Fig. S7, we show the photos of several MoS_2 sheets before and after the ablation. Changes in the color of the MoS_2 sheets are clearly seen after the ablation.

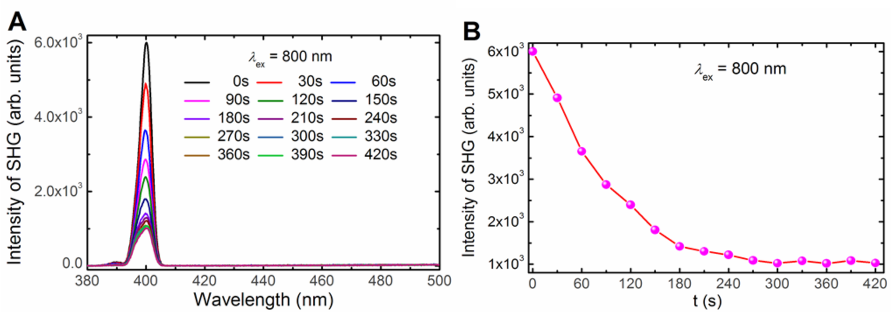

Fig. S6 (A) Evolution of the nonlinear response spectrum of a MoS_2 layer with increasing ablation time. The power of the fs laser light was 80 mW. (B) Dependence of the SHG intensity on the irradiation time of the fs laser light.

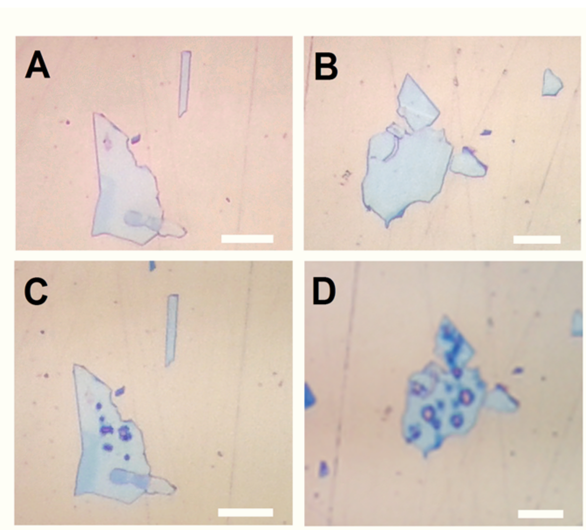

Fig. S7 Photos of the MoS_2 layers on the Au/SiO_2 substrate before ((A) and (B)) and after ((C) and (D)) the ablation by using fs laser light. The changes in the color at the ablated spots originating from the changes in the thickness of the MoS_2 layers are clearly seen. The length of the scale bar is 10 μm.

SI-8. Optical data storage realized in MoS_2 layers on the Au/SiO_2 substrate

By exploiting both the enhancement of SHG and the thickness dependence of SHG for the MoS_2 layers on the Au/SiO_2 substrate, we have demonstrated the optical data storage on the MoS_2 layers, as shown in Fig. S8. The recorded patterns can be extracted by either reading the SHG intensity of the MoS_2 layers or directly examining the color change if it is significant.

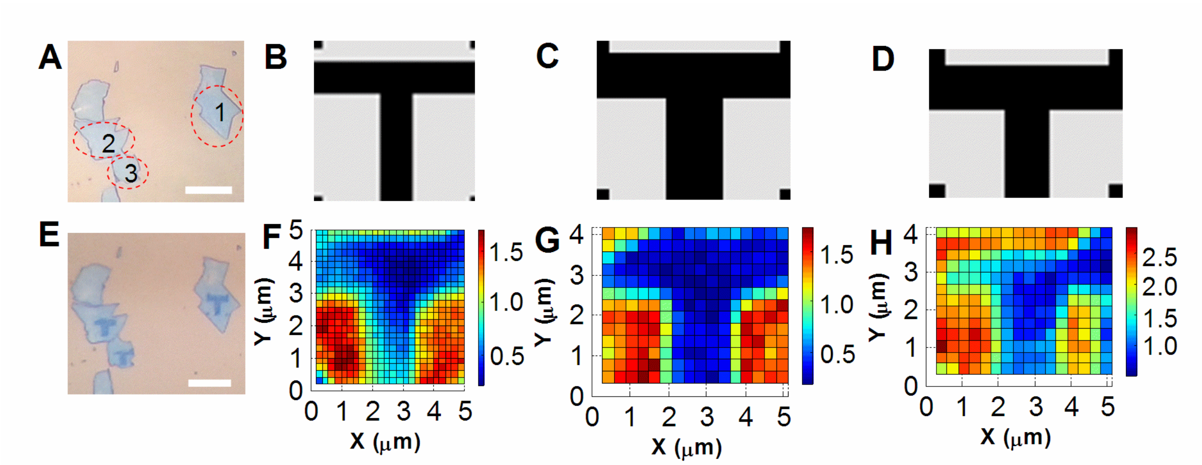

Fig. S8 Optical data storage demonstrated by using the MoS_2 layers on the Au/SiO_2 substrate. The photos of several MoS_2 sheets before and after the recording of patterns are shown in (A) and (E), respectively. The recorded data (letter "T") is clearly seen on the MoS_2 sheets because of the color change. (B)-(D) are three original patterns used for the data recording. (F)-(H) are the corresponding patterns extracted by reading the SHG intensity of the MoS_2 sheets. The length of the scale bar is 10 μm.

References

S1 R. A. Neville, and B. L. Evans, *Phys. Status Solidi B,* 1976, **73**, 597-606.

S2 C. C. Shen, Y. T. Hsu, L. J. Li, and H. L. Liu, *Appl. Phys. Express,* 2013, **6**, 125801.

S3 F. Bunting, Light Source Computer Images, Inc. An X-Rite Company, *The colorshop color primer*, 1998, pp 74-75.

S4 P. B. Johnson, and R. W. Christy, *Phys. Rev. B,* 1972, **6**, 4370-4379.

S5 E. D. Palik, *Handbook of Optical Constants of Solids*, Academic, New York, 1985.